Applied Chemical Engineering (2022) Volume 5 Issue 1
doi:10.24294/ace.v5i1.1450

Original Research Article

Effect of vulcanization and reaction temperature of the carbide supported on activated carbon on glycerol trioleate deoxygenation

Esneyder Puello-Polo*, Wendy Martinez Santiago, Brando Martínez Hernández, Vanessa Sarmiento Ramos, Alberto Albis Arrieta

Universidad del Atlántico, Barranquilla, Colombia. E-mail: esneyderpuello@mail.uniatlantico.edu.co

ABSTRACT

Cobalt molybdenum carbide supported on activated carbon was synthesized and the effect of sulfiding on the catalytic activity of the glycerol trioleate deoxygenation process (DOX) was evaluated. Prior to the glycerol trioleate deoxygenation reactions, the catalyst was reduced and sulfided with CS_2/H_2. The CoMo/CA carbide was characterized by specific area (B.E.T), X-ray diffraction (XRD), elemental analysis (CHON-S), potentiometric titration with n-butylamine and X-ray photoelectron spectroscopy (XPS). The specific area of the CoMo/CA carbide and the support were 246 m^2/g and 881 m^2/g, respectively. XRD analysis proved the presence of Co6Mo6C2 and metallic cobalt. XPS showed the presence on the surface of signals assignable to $Mo^{\delta+}$, Mo^{4+}, Mo^{6+}, Co^{2+}, S^{2-} and SO_4^{2-}. Sulfided CoMo/CA carbide showed higher activad to glycerol trioleate esoxygenation than unsulfided CoMo/CA carbide. The highest yield was obtained at 310 °C, 900 psi H_2 and 2 h of reaction (100% conversion) and a higher selectivity towards heptadecane (55%) and octadecane (45%) favoring decarboxylation (HDCX) and decarbonylation (HDCn) than hydrodeoxygenation (HDO).

Keywords: Sulfidation; CoMo/CA Carbide; Deoxygenation; Glyceryl Trioleate; HDO; HDC

ARTICLE INFO

Received: 18 January 2022
Accepted: 6 April 2022
Available online: 28 April 2022

1. Introduction

Recently, some processes have been proposed to extract biofuels from vegetable oil, some of which are biodiesel and green diesel[1]. The latter is effectively more energy-saving than biodiesel because its physicochemical properties are very similar to hose exhibited by fuels derived from petroleum[2].

The hydrotreating of oils of vegetable or animal origin to obtain biofuels with high added value has become an important process that heterogeneous catalysis has been studying. This process is not only limited to the purification of oil cuts, but also to the removal of oxygen present in fatty acids of vegetable or animal origin by means of DOX reactions, to obtain linear kerosenes such as common diesel[3]. The DOX reactions of these organic compounds can occur from three different pathways which are: direct hydrodeoxygenation (HDO), decarbonylation (HDCn) and decarboxylation (HDCx)[2]. Hydrotreating fatty acids from discarded edible oils is one of the main ways to obtain biofuels nowadays and thanks to the fact that it can be carried out under conditions similar to those of hydrotreating crude oil cuts, countries such as Brazil have developed co-processing units for common diesel and vegetable oils[3].

In this regard, Asikinmijan *et al*. obtained green diesel through cleaner catalytic deoxygenation of Jatropha oil by using multi-walled carbon nanotubes such as MWCNTs, Co/MWCNTs, Ni/MWCNTs and NiCo/MWCNTs. The results showed high catalytic activity for NiCo in the decarboxylation/decarbonylation routes with a total of 80% saturated and unsaturated hydrocarbon in the range of C18 and C17, high selectivity towards C15 and C17 hydrocarbons[4]. Sanchez *et al*. evaluated the effect of two Ni-Mo type catalysts supported on Al_2O_3 in the deoxygenation process of higuerilla oil, for the production of renewable diesel. The highest mass yield towards renewable diesel (C9-C24) of 82.9% was obtained with the synthesized catalyst containing 4.5% NiO and 20% MoO_3[1].

Recently, transition metal carbides, especially molybdenum carbide, have been used in this type of processes. Hence, Teixeira[5], evaluated the hydrotreating of sunflower oil using supported molybdenum carbide (β-Mo_2C/Al_2O_3). The results suggest that the total transformation of triglycerides to linear alkanes proceeds in two steps: (i) thermal cracking of triglycerides forming free fatty acids, (ii) hydrogenation of the double bonds and the carboxylic group of the free fatty acid forming n-alkanes, no CO and/or CO_2 formation was detected, implying that decarbonylation and/or decarboxylation routes do not play an important role when molybdenum carbide is used. Han, Duan, *et al.*[6], found that the conversion of methyl palmitate with 5% catalyst was 67% and selectivity of 92% towards hydrocarbons, by increasing the amount of catalyst to 10% a conversion of 90% was achieved, indicating that the high loading of active components are related to the amount of active sites.

In 2018, Wang, Jiang, *et al.*[7], performed vegetable oil hydrotreating over different catalysts to produce green diesel. Molybdenum carbide supported on activated carbon (Mo_2C/AC) was shown to be the catalyst with the best catalytic activity, 100% conversion and 21.01% cracking ratio, compared to MoO_3/Al_2O_3 (85.64%, 25.79%), MoS_2/Al_2O_3 (83.46%, 11.88%), Mo/Al_2O_3 (67.99%, 33.19%), Ni_2P/Al_2O_3 (48.72%, 3.49%), Ni/Al_2O_3 (18.12%, 0.00%) and MoO_3/AC (56.05%, 18.55%) catalysts. XRD, XPS and N_2 adsorption-desorption results showed that the coke deposited on the catalyst surface and the formation of MoO_2 and MoO_3 led to deactivation at the end of the reaction. Therefore, research is aimed at the synthesis of catalysts using transition metal carbides to maximize the yield in the hydrodeoxygenation processes of vegetable oils or unsaturated fatty acids. For this reason, the purpose of this work was to evaluate the effect of sulfur and temperature modification on the catalytic activity of triolein hydrogenation to obtain hydrocarbons using a bimetallic Co-Mo carbide supported on activated carbon.

2. Experimental methodology

2.1 Synthesis of supports and catalytic precursors

2.1.1 Synthesis of cobalt-molybdenum precursor supported on activated carbon (CoMo-C/CA).

The bimetallic precursors supported on activated carbon (Merck: 899 m^2/g, 0.57 cm^3/g, 7.95 nm), were prepared by the co-precipitation method at pH 7. The activated carbon was impregnated with the aqueous solutions of ammonium heptamolybdate heptahydrate (Sigma Aldrich, 98%) and cobalt nitrate hexahydrate (Sigma Aldrich, 98 %) in a stoichiometric ratio of Co/(Co + Mo) = 0.25 (12 %p/p Co and 20 %p/p Mo). Subsequently, the obtained suspension was stirred at 80 °C for 2 h and once the impregnation time had elapsed, the solvent was removed by evaporation and immediately dried at 110 °C for 12 h[8].

2.1.3 Synthesis of cobalt-molybdenum carbides supported on activated carbon (CoMo-C/CA)

The carburized cobalt-molybdenum phase supported on activated carbon was prepared by the carbothermal reduction method with hydrogen, in a vertical electric furnace with temperature controller (Electro Salgado Ltda.), in which a stainless steel reactor with a quartz fiber bed was placed with the Co-Mo precursor and 100 mL/minute of H_2 was passed through it, heating up to 700 °C at 5 °C/minute. Once the temperature was reached, it was held for 1 hour and then cooled to room temperature, where it was passivated with 50 mL/min of air(1%vol)/N_2[8].

2.2 Characterization of catalytic precursors

Different characterization techniques were performed in order to determine the physicochemical properties of the synthesized solids and their relationship with the catalytic activity:

2.2.1 Textural properties: Specific area (SBET), pore diameter (PD) and pore volume (PV)

This analysis technique allowed to know the available adsorption area of the catalyst. The BET method was used to determine the specific area, which is based on the physical adsorption of a gas to which the adsorbed volume is determined in equilibrium at a temperature close to that of liquefaction and in a relative pressure range between 0.1 and 0.3, while the pore diameter and volume were calculated by the Horvath-Kawazoe method[9]. The textural properties were determined by N_2 adsorption at –196 °C using a Micromeritics ASAP 2010 sorptometer. Prior to the measurements the samples were degassed at 300 °C for 16 hours in a vacuum of 10-3 Torr.

2.2.2 X-ray diffraction (XRD)

X-ray diffraction analysis was used to obtain information on the crystalline phases present in the precursors and carburized solids. This analysis was performed on a SIEMENS D-5005 diffractometer using the K radiation source of Cu (1.5456 Å), taking the scanning angle was $10° \leq 2\theta \leq 90°$ at a step size of 0.02° and an acquisition rate of 0.08°/s. The identification of the different phases was done by comparing the experimentally obtained diffraction patterns with the JCPDS library diffraction patterns[10].

2.2.3 X-ray photoelectron spectroscopy (XPS)

This method provides information about the atomic composition, chemical environment and oxidation state of the metals constituting the catalyst surface. The surface composition of the carbides was determined with a VG-ESCALAB model 220 i-XL photoelectron spectrometer with a dual Mg/Al anode (non-monochromatic), operated at 400W. Aluminum K radiation (1486.6 eV) was used in the analyses reported in this paper. All measurements were run at UHV (less than 10^{-8} Torr), and instrument calibration was done employing the $4f_{7/2}$ line of Au (83.9 eV).

Quantification of the XPS signals and curve fitting of the spectra was carried out with XPS PEAK 4.1 and XPS GRAPH after baseline subtraction using the Shirley method. The combination of 80% Gaussian-20% Lorentzian and tabulated atomic sensitivity factors were typically used. To minimize loading effects the dominant peak of the C1s spectrum of the support at 284.6 eV was used as internal reference. The reported binding energies were accurate to within 0.2 eV.

2.2.4 CHNO-S elemental analysis

Elemental analysis was used to determine the sulfur content present in the carburized and pre-sulfurized solids. This analysis was carried out by thermal oxidation at 1,000 °C and by chromatographic separation of the resulting gases, using an EA 1108 Thermo (Carlo Erba) CHNS-O equipment.

2.2.5 Acidity test

Potentiometric titration with n-butylamine made it possible to determine the strength and amount of acid sites in the solids. In this test, a solution of 50 mL of acetonitrile (Merck, 99%) in 200 n-butylamine (Merck, 0.1 N) and 100 mg of the catalyst was prepared in a beaker, immediately titrated and the first reading (mV) was recorded with a Laqua potentiometer, indicating the maximum acid strength of the sample. Then, the neutralization of the sites was carried out until the final point of the titration, when the electrode potential was constant with the addition of the titrating solution.

2.3 Thiophene hydrodesulfurization catalytic activity measurements

All catalytic experiments were carried out in a batch reactor equipped with a mechanical stirrer and an arrangement for collecting liquid samples during the experiment.

2.3.1 Activation of the carbide CoMo-C/CA

1.0 g of carbide was activated by sulfidation in a continuous flow reactor of 30 cm long × 2 cm internal diameter, in a tubular furnace equipped with a temperature controller (Electro Salgado Ltda). With a flow of 50 mL/min of H_2 and a current of CS_2/Heptane at 2%. Then, after cooling the solid to

room temperature, the necessary amount of catalyst was taken and stabilized in heptane.

The sulfided and unsulfided carbide were identified as CoMo-C/CA-S and CoMo-C/CA-NS, respectively.

2.3.2 Reaction of sulfided CoMo-C/CA with trioleate solution in cyclohexane and tetrahydronaphthalene

300 mg of the catalyst was mixed with 80 ml of 2% solution of glycerol trioleate (Sigma Aldrich, 65%) in Cyclohexane (Sigma Aldrich, 99.5%) - Tetrahydronaphthalene (Merck, 99%), in the batch reactor and, purged with N_2 and pressurized with H_2 at 300 psi. Then, it was heated to 250, 280 and 350 °C up to 900 psi H_2 final pressure and 350 rpm stirring, respectively. Samples were taken at 1 and 2 hours after the reaction reached the indicated temperature. For the identification of reactant and reaction products, agilent technologies 7890B GC System 5977A MSD GC-MS was used. As a comparison, a catalytic test was performed with unsulfided CoMo-C/CA carbide.

3. Analysis and discussion of results

3.1 Characterization of CoMo-C/CA carbides

3.1.1 Textural properties: specific area (S_{BET}), pore diameter (PD) and pore volume (PV) of CoMo-C/CA carbide

Figure 1 shows the isotherms of CA and CoMo-C/CA carbide, which is type I according to IUPAC classification, characteristic of microporous solids ($0 < P_D < 2$ nm) that have small external surfaces and whose adsorption limit is given by the micropore volume versus pore size[11]. The pore volume of the carbide is 0.26 cm^3/g with respect to the support 0.66 cm^3/g, which value is lower, due to the presence of the supported metals on the catalyst, which can migrate into the pores during the synthesis (see **Table 1**).

The inset of **Figure 1**, shows the pore size distribution curve evaluated by the Horvath-Kawazoe method, with a narrow unimodal distribution between 0.51–0.69 nm for the activated carbon and 0.51–0.73 nm with a pore diameter of 0.54 nm for CoMo-C/CA, which reflects the geometrical shape of the pores, these being of slit type characteristic of

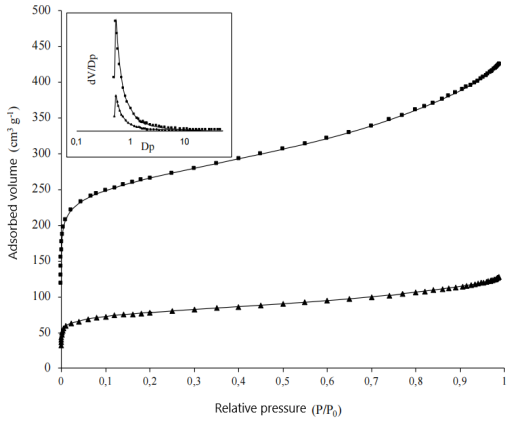

Figure 1. Adsorption isotherms of N_2 and pore size distribution on the activated carbon and CoMo-C/CA carbide. Activated carbon (■), CoMo-C/CA (▲).

Table 1. Textural properties of activated carbon and CoMo-C/CA carbide

Catalyst	Specific area (m^2/g)	Pore volume (cm^3/g)	Pore diameter (nm)
Activated carbon	881	0.66	0.94
CoMo-C/CA	246	0.26	0.54

activated carbons[11].

3.1.2 X-ray diffraction of CoMo-C/CA carbides

Figure 2 shows the XRD patterns obtained allowed to appreciate the formation of the bimetallic $Co_6Mo_6C_2$ phase (JCPDS 800339[11]) with diffraction peaks at 2θ(º) = 35.7, 40.3, 42.8, 46.6 and a metallic cobalt phase (JCPDS 15-0806[11]) with signals at 2θ(º) = 44.0, 51.9 and 76.1. The diffraction peaks were narrow and defined with respect to the background, which allows assuming that the materials possess high crystallinity. On the other hand, once the activation by sulfidation was performed, it was observed that there were no changes in the crystalline phase of the carbide as confirmed by Puello *et al*. in other studies where the changes occur at the surface level[12].

3.1.3 X-ray photoelectron spectroscopy of CoMo-C/CA carbides

Figure 3 shows the XPS spectra $Mo3d_{5/2\text{-}3/2}$, Co $2p_{3/2\text{-}1/2}$ and S $2p_{3/2\text{-}1/2}$. For $Mo3d_{5/2\text{-}3\text{-}3/2}$, it corresponds to the binding energy between 220 eV and 240 eV, where the signals of the sulfided and unsulfided carbide can be assigned to the carburized phase ($Mo^{\delta+}$

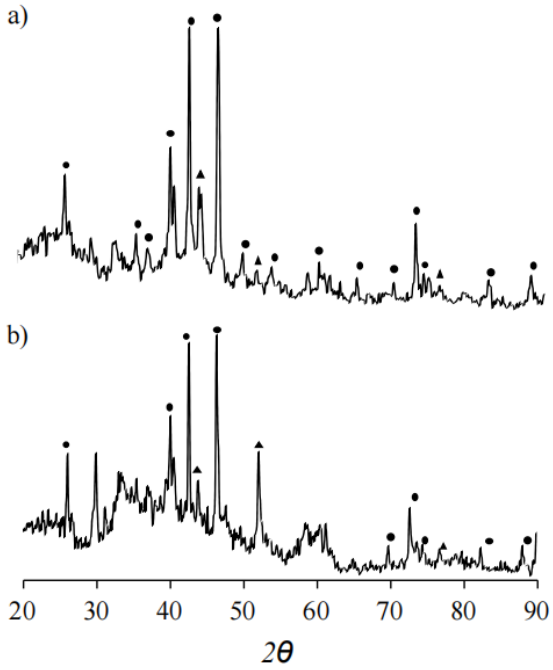

Figure 2. X-ray diffraction patterns of CoMo-C/CA-NS (a) and CoMo-C/CA-S (b) carbides. $Co_6Mo_6C_2$ (●), Co (▲).

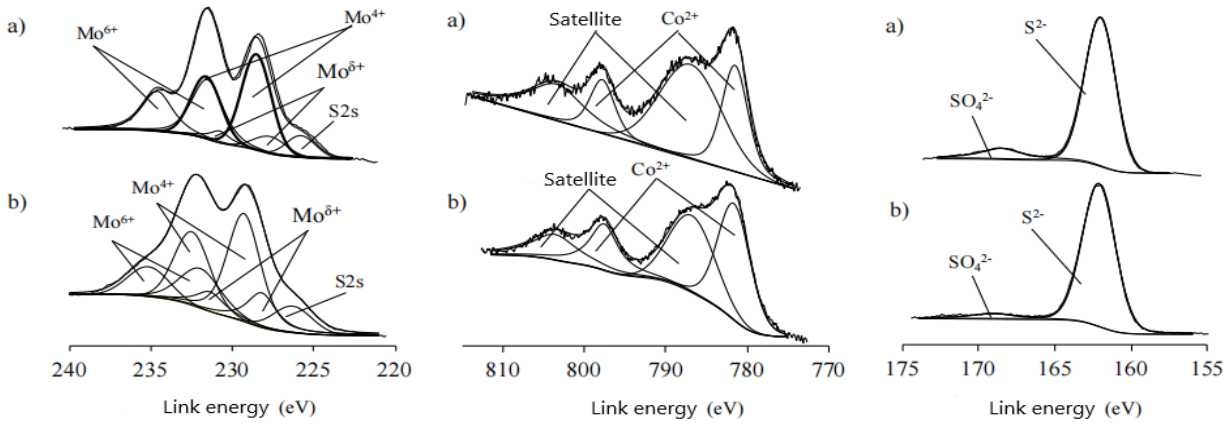

Figure 3. X-ray photoelectron spectra Mo 3d, Co 2p and S 2p regions of sulfiding and no sulfiding CoMo/CA carbide: a) CoMo-C/CA-NS, b) CoMo-C/CA-S.

($0 \leq \delta \leq 2$)) between 228.5–231.1 eV, oxycarbide (Mo^{4+}) between 229.0–232.4 eV and molybdenum trioxide (Mo^{6+}) between 232.3–235.5 eV[13]. In addition, the XPS $Mo3d_{5/2\text{-}3/2}$ spectrum reveals for the non-sulfided carbide the presence of sulfur on the surface due to the shoulder in the spectrum at 226.5 eV, this result is because the precursor CoMo/C. A is obtained from $CoSO_4$ and because it is activated cabon its support is not subjected to a calcination process but to a carburization process[13]. To evaluate the presence of sulfur in the sulfurized and non-sulfurized carbide, the S 2p spectrum shown in **Figure 4** was analyzed, where two signals are observed in the intervals 161.8 eV–168.9 eV, corresponding to sulfide (S^{2-}) and sulfate (SO_4^{2-})[13]. The spectrum in the Co 2p region in the sulfided and unsulfided carbide (**Figure 5**), showed two peaks between 781.1–796.9 eV and 781.4–797.1 eV assignable to Co^{2+} species and a satellite peak around 787.0 eV and 803.0 eV[13], corroborating the presence of CoMoO4 on the surface, which can be observed to decrease this oxidic phase upon sulfiding due to the generation of "CoMoS"[14].

Table 2 shows the atomic percentages of each element determined by XPS analysis of the sulfided and unsulfided CoMo/CA carbide, showing the effect of sulfiding that increases the presence of cobalt on the surface with a higher proportion of sulfide, due to the increase in the amount of sulfur on the support area.

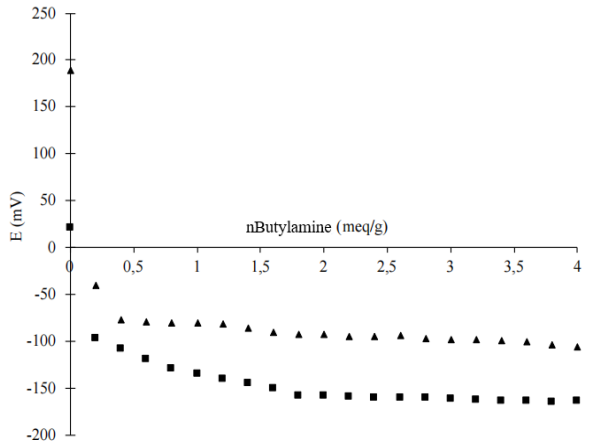

Figure 4. Potentiometric titration with n-butylamine of (▲) sulfiding and (■) no sulfiding CoMo/CA carbides.

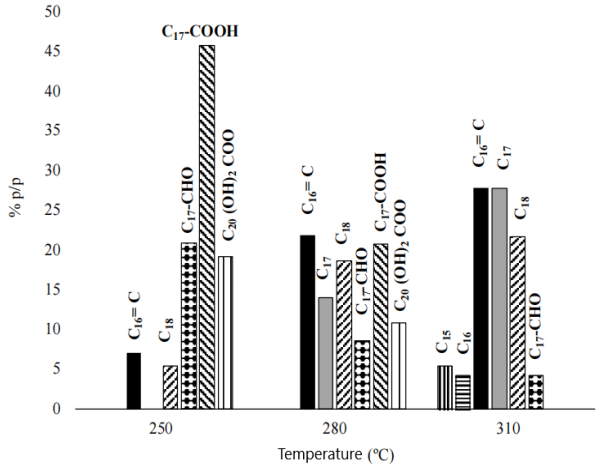

Figure 5. Glyceryl trioleate DOX conversion to reaction products of sulfiding CoMo/CA carbides at 250 ºC, 280 ºC and 310 ºC in 1 h.

Table 2. Composition of Mo, Co and S by XPS (as atomic %) and chemical analysis (CHONS) of sulfiding and no sulfiding CoMo/CA carbide

Catalyst	XPS Analysis (as atomic %)			Elemental analysis CHONS (% p/p)
	Mo	Co	S	S
CoMo-C/CA-NS	3.13	2.80	5.51	3.02
CoMo-C/CA-S	2.60	9.39	9.90	13.8

3.1.4 Acidity test with nButylamine

Figure 4 shows the neutralization profile for the unsulfided CoMo-C/CA carbide with an initial potential value of 189.8 mV and 21.2 mV for the sulfided CoMo-C/CA carbide, which according to the classification reported by Cid and Pechi[15], correspond to very strong surface acid sites present in the catalyst. As for the concentrations of acid sites per gram of catalyst, 0.6 meq/g was observed for the non-sulfided carbide and 1.8 meq/g for the sulfided carbide. This behavior demonstrates the influence of sulfiding the carbide because it decreases the acid strength and increases the amount of acid sites.

3.2.1 Catalytic activity of sulfided and unsulfided CoMo-C/CA carbide in the hydrogenation reaction of glyceryl trioleate

The analyses performed by GC-MS chromatography showed the presence of hydrocarbons in the hydrogenation reaction of glyceryl trioleate, using the sulfided and unsulfided CoMo-C/CA catalyst. In **Figures 5** and **6**, the mass percentages of linear kerosenes (C_{15}-C_{18}), alkenes (C_{16}=C), aldehydes (C_{17}CHO), unsaturated fatty acids (C_{17}COOH) and fatty acid ester compounds ($C_{20}(OH)_2COO$) can be seen.

Taking into account the time in which the different reactions were carried out, it was possible to appreciate an increase in the concentration of n kerosenes C15 to C18 proportional to the increase in temperature, evidencing that at 310 °C the fatty acids derived from glycerol trioleate such as glycerol mono-oleate ($C_{20}(OH)_2COO$) and oleic acid (C_{17}COOH) are totally consumed, resulting in a total conversion (100%) of the triglycerides to hy-

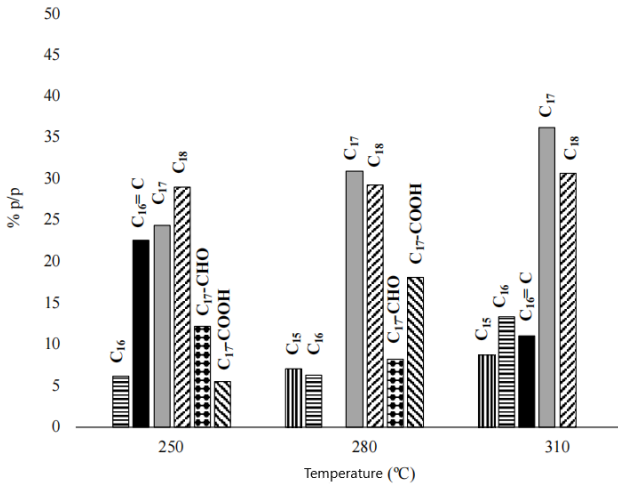

Figure 6. Glyceryl trioleate DOX conversion to reaction products of sulfiding CoMo/CA carbides at 250 ºC, 280 ºC and 310 ºC in 2 h.

drocarbons.

A comparison of the hydrogenation of glycerol trioleate with unsulfurized CoMo-C/CA carbide at 310 ºC showed that it produces low n-paraffin production and a high percentage of unsaturated hydrocarbons, which may be related to the low number of acid sites (see **Table 3**).

3.2.2 Performance and selectivity at C_{17} and C_{18}, using the sulfided and unsulfided CoMo-C/CA carbides

Pentadecane (C_{15}) and hexadecane (C_{16}) presented low concentrations in comparison with octadecane and heptadecane. For this reason, the yield and selectivity are expressed in terms of the desired products heptadecane and octadecane, since they are the two alkanes with the highest number of carbon atoms in their fatty acid molecules and of high interest for generating renewable diesel[16]. **Figure 7** shows that octadecane presents higher yield and selectivity in the reaction at 250 °C of sulfurized CoMo-C/CA carbide, this would be related to the acid sites that allow the hydrogenation of the C-O bond of fatty acids, indicating that it is facing a hydrodeoxygenation reaction. On the other hand, as the reaction temperature increases, there is an increase in yield and selectivity towards heptadecane which favors decarbonylation and decarboxylation as shown in **Figures 7** and **8**, and **Table 3**.

Considering the main hydrocarbons obtained (n-heptadecane and n-octadecane), the possible reaction routes by which they were formed can be determined: hydrodeoxygenation (HDO), decarboxylation (HDC_X) and decarbonylation (HDC_n) as shown in **Figure 9**[17].

According to **Figure 9**, the formation of kerosenes followed three catalytic mechanisms HDO, HDC_n and HDC_x, and the most efficient route will be the one that generates saturated hydrocarbons with the highest percentage yield. The HDO route allowed the elimination of oxygen as water, where oleic acid is dehydrated until obtaining octadecanal ($C_{17}CHO$), this aldehyde is saturated producing octadecanol, and then deoxygenated obtaining the unsaturated isomer (octadecene) and dehydrated producing octadecane. The decarbonylation process (HDCn) proves that the heptadecane compound can be generated in two ways. In the first reaction the unsaturated compound is reduced to heptadecane by elimination of CO, generating a product with one less carbon than the original fatty acid; while in the second pathway the aldehyde loses two hydrogens forming the heptadecene molecule until heptadecane is obtained. Finally, the decarboxylation reaction

Table 3. Reaction products composition at 310 ºC of sulfiding and no sulfiding CoMo/CA carbides

Reaction Products	Sulfide-310 ºC		No Sulfurized-310 ºC	
	1 h	2 h	1 h	2 h
C_{15}	5.5	8.7	0.0	4.4
C_{16}	4.3	13.4	0.0	0.0
$C_{16}=C$	27.9	11.0	0.0	0.0
C_{17}	27.8	36.3	4.8	12.2
C_{18}	21.7	30.7	5.7	12.3
C_{17}-CHO	4.3	0.0	10.8	12.2
C_{17}-COOH	0.0	0.0	70.1	53.8
C_{20}(OH)2COO	0.0	0.0	75.0	59.2

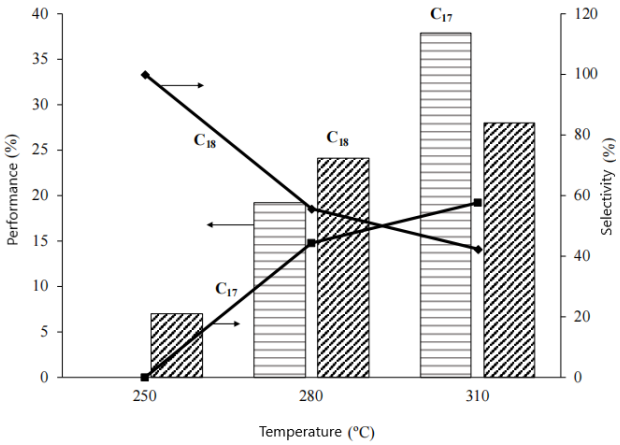

Figure 7. Effect of the temperature on yield and selectivity of C_{17} and C_{18} at 1 h using sulfided CoMo/CA carbide.

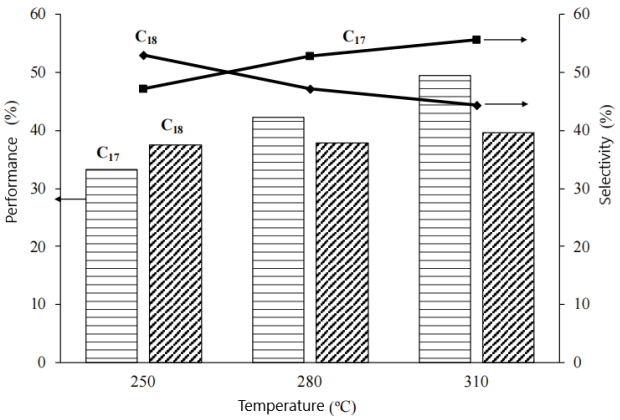

Figure 8. Effect of the temperature on yield and selectivity of C_{17} and C_{18} at 2 h using sulfided CoMo/CA carbide.

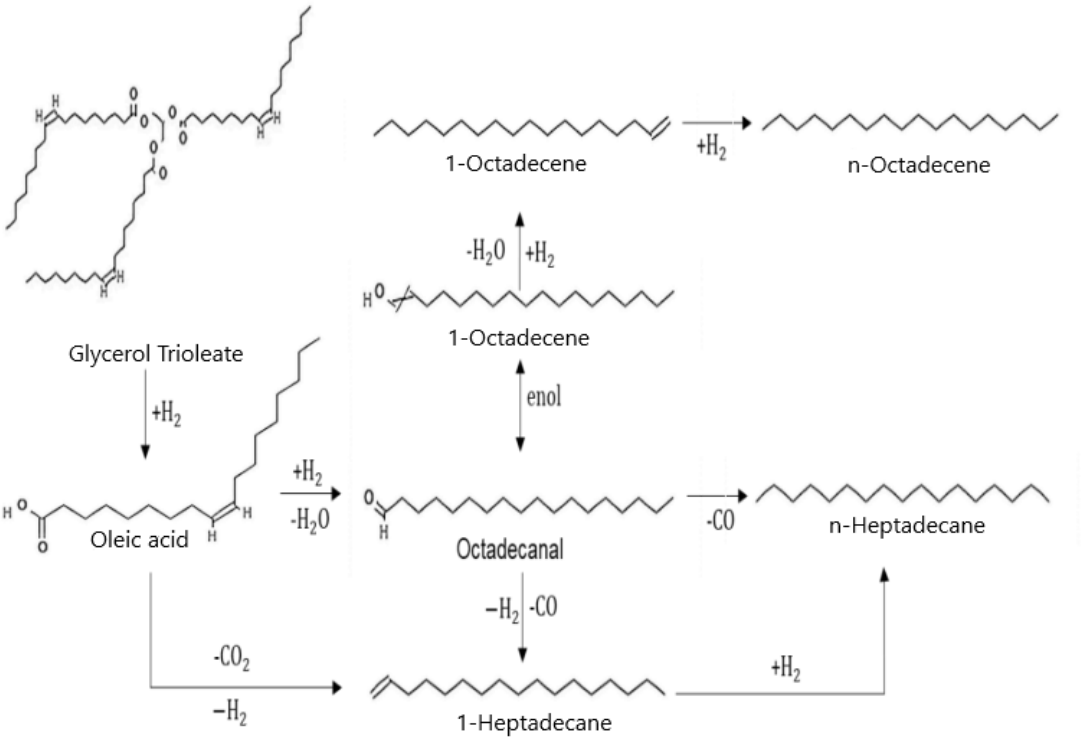

Figure 9. Reaction pathways for glyceryl trioleate deoxygenation using sulfided CoMo/CA carbide.

(HDCx) is simplified directly by the elimination of oxygen as CO_2, being reduced to heptadecene by the loss of hydrogen which then hydrogenates forming heptadecane as the final product[16].

3.2.3 Proportion of each reaction route: HDO, HDCN and HDCX in the hydrogenation of glycerol trioleate

In order to calculate the degree of participation of each type of reaction in the overall process it is convenient to define some parameters that allow some numerical estimations. If it is considered that the content of hydrocarbons with the same chain length as the fatty acids of the starting material (C_{16} and C_{18}) is indicative of the occurrence of HDO, the degree of participation of this reaction in the conversion of hydrocarbons can be estimated by equation 1[18].

$$\%\ HDO=\frac{C_{18}+C_{16}}{(C_{18}+C_{16})+(C_{17}+C_{15})}\times 100 \qquad (1)$$

Similarly, the percentage represented by the two reactions characterized by decreasing the chain length of the starting fatty acid chains (HDC) by one carbon atom can be estimated from the C_{15} and/or C_{17} hydrocarbon content (Equation 2)[18]. C_{17} + C_{15}

Where:

HDC= HDC + HDC

$$\%\ HDC=\frac{C_{17}+C_{15}}{(C_{18}+C_{16})+(C_{17}+C_{15})}\times 100 \qquad (2)$$

Table 4 shows that at 250 ºC a higher conversion to HDO was obtained, while between 280 and 310 °C for the sulfided CoMo-C/CA carbide did not show an appreciable difference between HDO and HDC as did the non-sulfided CoMo-C/CA carbide. The differences between catalysts and reaction pathways can be related to the number and strength of acid sites. It is evident that, the higher proportion

Table 4. HDO and HDC conversion for glyceryl trioleate deoxygenation using sulfided and no sulfide CoMo/CA carbide

T (ºC)	Sulfide CoMo-C/CA		Non Sulfide CoMo-C/CA	
	% HDO	% HDC	% HDO	% HDC
250	59,0	41,0	-	-
280	48,3	51,7	-	-
310	49,5	50,5	42,5	57,5

of heptadecane in indicates that the endothermic HDC pathways are favored with increasing temperature as reported by Gosselink[19] and Toba[20], suggesting that the best conditions for fatty acid deoxygenation reactions is around 300 ºC.

4. Conclusions

• The specific area of the CoMo-C/CA carbide was 246 m^2/g and of the activated carbon support 881 m^2/g with average pore diameter of 0.54 nm for a slit-like pore shape characteristic of activated carbons.

• XRD analysis verified the presence of the bimetallic phase $Co_6Mo_6C_2$ and metallic cobalt.

• XPS revealed on the surface of the material the species $Mo^{\delta+}$, Mo^{4+}, Mo^{6+}, Co^{2+}, S^{2-} and SO_4^{2-} with higher proportion of sulfur and cobalt for the sulfided carbide.

• Potentiometric titration with nButylamine showed that sulfidation decreases the strength and number of acid sites by 189.8 mV vs. 21.2 mV and 0.6 meq/g vs. 1.8 meq/g, respectively.

• The best yield and selectivity towards renewable diesel was obtained at 310 °C and 2 h of reaction.

The hydrocarbon with the highest yield and selectivity was heptadecane with 45% and 55%, followed by octadecane at 28% and 45%, indicating that the products were formed in higher proportion by the routes (HDC_n + HDC_x), than by HDO, which is related to the strength and number of acid sites.

Conflict of interest

Authors declared no conflict of interest.

Acknowledgements

The authors would like to thank the Universidad del Atlántico for the call for research equity and the 1st internal call for support for the development of undergraduate and graduate research projects.

References

1. Sanchez L, Llano B, Rios L. Production of renewable diesel from Higuerilla oil using Nickel-Molybdenum catalysts supported on alumina (in Spanish). Technological Information 2017; 28(1): 13–24.
2. De la Rosa EA. Hydroprocessing of jatropha Curcas L. vegetable oil for the production of green fuels [Master's Thesis] (in Spanish). National Polytechnic Institute of Mexico. 2013.
3. Aparicio A, Melgarejo E. Kinetics of the HDO reaction of vegetable oil to obtain biofuels [Master's Thesis] (in Spanish). Universidad Central de Venezuela; 2018.
4. Asikimijan N, Lee H, Abdulkareem-Alsultan G, *et al*. Production of green diesel via cleaner catalytic deoxygenation of Jatropha curcas oil (in Spanish). Journal of Cleaner Production 2016; 167: 1048–1059.
5. Sousa LA, Zotin JL, Teixeira da Silva V. Hydrotreatment of sunflower oil using supported molybdenum carbide. Journal Applied Catalysis A: General 2012; 449: 105–111.
6. Han J, Duann J, Chen P, *et al*. Carbon-supported molybdenum carbide catalysts for the conversion of vegetable oils. ChemSusChem 2012; 5(4): 727–733.
7. Wang F, Jiang J, Wang K, *et al*. Activated carbon supported molybdenum and tungsten carbides for hydrotreatment of fatty acids into green diesel. Fuel 2018; 228: 103–111.
8. Puello-Polo E, Gutiérrez-Alejandre A, González G, *et al*. Relationship between sulfidation and HDS catalytic activity of activated carbon supported Mo, Fe–Mo, Co–Mo and Ni–Mo carbides. Catalysis Letters 2010; 135(3–4): 212–218.
9. Horvarth GK. Method for the calculation of effective poro size distribution in molecular sieve carbon. Journal of Chemical Engineering of Japan 1983; 16(6): 470–475.
10. Power Diffraction File, ICDD. Newtown Square, Philadelphia, USA. 1995.
11. Sing KSW, Everett DH, Haul RAW, *et al*. Reporting physisorption data for gas/solid systems with special reference to the determination of surface area and porosity (Recommendations 1984). Pure and Applied Chemistry1985; 57(4): 603–619.
12. Puello-Polo E, Ayala-G M, Brito JL. Sulfidability and thiophene hydrodesulfurization activity of supported NiMo carbides. Catalysis Commu-

nications 2014; 53: 9–14.
13. Puello-Polo E, Brito JL. Effect of the type of precursor and the synthesis method on thiophene hydrodesulfurization activity of activated carbon supported Fe-Mo, Co-Mo and Ni-Mo carbides. Journal of Molecular Catalysis A: Chemical 2008; 281: 85–92.
14. Topsoe NY, Topsoe H. Characterization of the structures and active sites in sulfided Co-$MoAl_2O_3$ and $NiMoAl_2O_3$ catalysts by NO chemisorption. Journal of Catalysis 1983; 84(2): 386–401.
15. Cid R, Pechi G. Potentiometric method for determining the number and relative strength of acid sites in colored catalysts. Applied Catalysis 1985; 14: 15–21.
16. Arora P, Ojagh H, Woo J, *et al*. Investigating the effect of Fe as a poison for catalytic HDO over sulfided NiMo alumina catalysts. Applied Catalysis B: Environmental 2018; 227: 240–251.
17. Hancsók J, Eller Z, Polczmann G, *et al*. Sustainable production of bioparaffins. Chemical Engineering Transactions 2013; 35: 1027–1032.
18. Volonterio E, Bussi J, Castiglioni J, *et al*. Catalytic hydrotreating of vegetable oils for the production of liquid biofuels. Magazine of the Technological Laboratory of Uruguay 2017; 14: 37–43.
19. Hollak S, Gosselink R, Van Es D, *et al*. Comparison of tungsten and molybdenum carbide catalysts for the hydrodeoxygenation of oleic acid. ACS Catalysis 2013; 3(12): 2837–2844.
20. Tobam M, Abe Y, Kuramochi H, *et al*. Hydrodeoxygenation of waste vegetable oil over sulfide catalysts. Catalysis Today 2010; 164(1): 533–537.